

## RESULTS OF THE FIRST THIRTY FOOT DROP TEST OF THE MOSAIK KfK CASK\*

K. B. Sorenson, R. Salzbrenner, G. Wellman, W. Uncapher, J. Bobbe  
Sandia National Laboratories \*\*  
P.O. Box 5800  
Albuquerque, NM, 87185

### ABSTRACT

The MOSAIK KfK cask, a ductile cast iron (DCI) nuclear material transportation cask donated to Sandia by Gesellschaft fur NuklearService (GNS), was drop tested on June 25, 1990 in Albuquerque, New Mexico. Conditions of the test were; 1) a 30 ft. drop without impact limiters onto an unyielding target, 2) cask metal temperature 16 F or below, and 3) a 0.75 inch deep flaw machined into the cask wall at the location of the highest tensile stress. The drop test was successful as judged by inspection of the machined flaw which showed no crack initiation.

This drop test, the first in a series, was designed to demonstrate the viability of using a fracture mechanics approach to design casks fabricated from ferritic materials (i.e., ferritic steels and DCI). In addition, the test demonstrated that a DCI cask can withstand severe impacts under accident-type conditions without failing in a brittle mode.

The drop test parameters were designed to produce high decelerations and yield-level stresses in the cask wall. The measured rigid body deceleration was approximately 800 gs. This compares with decelerations of 100 to 300 gs for drop tests of casks with impact limiters. The time to peak load was 1.2 to 2.8 msec., compared to 20 to 40 msec for casks dropped with impact limiters. The maximum strain during the drop test was 1400 microstrain (measured near the ends of the cask), which equates to a maximum tensile stress of about 37000 psi. This level of stress slightly exceeds the static yield strength and is about 80% of the dynamic yield strength. The test results of this initial drop test are discussed in detail in this paper.

### INTRODUCTION

The U.S. Department of Energy / Office of Environmental Restoration and Waste Management, through it's Transportation Technology Department, is sponsoring an effort to develop a fracture mechanics design approach for nuclear material transportation casks. The objective of this effort is to provide a sound technically based design methodology for structural ferritic material. Ductile cast iron (DCI) is used in this program because it is readily available and economical to test (relative to steels), is a candidate material for new cask designs in the U.S., and has precedence of certification for transport in Europe.

Gesellschaft fur NuklearService (GNS), a cask producer in Germany, donated two DCI casks to Sandia for test purposes. The two casks, the MOSAIK KfK and the MOSAIK I, are designed to ship low level nuclear waste. The DCI cast iron used in these casks serves as the structural containment boundary and conforms to ASTM specification A 874 [1], which is the material specification for low temperature service. The MOSAIK KfK was the test article for this program. The MOSAIK I was used for test instrumentation, rigging, and experimental drop test procedures development.

The drop test program is designed to verify that the linear-elastic fracture mechanics (LEFM) design approach is applicable to cask design. The fundamental equation is given by;

$$K_I = C\sigma(\pi a)^{1/2} \quad (\text{Eq. 1})$$

Where,  $K_I$  is the applied stress intensity ( $\text{ksi-in}^{1/2}$ ),

$C$  is a geometric constant,

$\sigma$  is the applied tensile stress (ksi), and

$a$  is the depth of an existing flaw.

In order to prevent crack initiation, the stress intensity,  $K_I$ , must be less than the fracture toughness of the material which is designated as  $K_{Ic}$ . The components of this test program involve the three parameters described in Eq. 1.

The purpose of this first test was to verify the LEFM design by demonstrating that a sub-critical flaw would not initiate (i.e. the crack would not extend) as a result of the drop tests. Additional tests will be performed with iteratively deeper flaws until initiation occurs. This sequence of tests will be used to quantify the margin of safety.

\* This was work performed at Sandia National laboratories, Albuquerque, New Mexico, supported by the U.S. Department of Energy under contract DE-AC04-76DP00789.

\*\* A United States Department of Energy Facility.

## TEST CASK DESCRIPTION AND DROP TEST CONDITIONS

The MOSAIK KfK cask, in the drop test orientation, is shown in Figure 1a. The cask weighs 14130 lbs., is 54 inches long and has a cavity diameter of 25 inches with a wall thickness of 8.4 inches.

The cask was dropped from a height of 30 ft. without impact limiters onto an unyielding target. The cask was in a horizontal position with mild steel rails attached near the two ends. The purpose of the rails was to enhance the effect of the impact by producing yield level stresses in the vicinity of the flaw as well as producing a through-wall tensile stress component. This drop test is an enhancement over regulatory drop test requirements as stated in 10CFR71 [2] since no impact limiters were used to mitigate peak level stresses and loading rates. Further, normal side impacts may not be expected to produce either yield stresses or the tensile stress field (through-wall) which may be required to propagate a flaw through the cask wall. The cask metal temperature was a maximum of -16 F at the time of the drop which was slightly higher than the 10CFR71 maximum temperature of -20°F.

The flaw machined into the cask for this first drop test was 0.75 inches deep with an aspect ratio of 3:1. The flaw was located on the cask surface at the longitudinal midpoint to coincide with the maximum applied tensile stress. Fig. 1b shows the details of the flaw.

## MATERIALS CHARACTERIZATION

A complete set of mechanical properties of the MOSAIK KfK cask was determined from a coring taken from the bottom of the cask. The coring was 16 inches in diameter and 8.5 inches thick. In order to quantify the effects of the microstructural variations through the thickness, the coring was sectioned into five (approximately equally spaced) "planes," each with a thickness of approximately 1 inch. This material was designated as Plane 1, starting at the inner cask wall, through Plane 5 at the outer cask wall. Tensile and fracture toughness specimens were machined from each "plane," and were tested in accord with ASTM Standard Test Methods [3,4]. The tensile tests were conducted at -20°F (which corresponds to the regulatory drop test temperature) at strain rates of  $10^{-3}$  and  $10^0$  per second. Static rate fracture toughness tests were performed at -20°F. Microstructural and composition measurements were made directly on the remnants of the mechanical test specimens. These standard test results and metallographic/compositional measurements are summarized\* in Table I.

In addition to the standard mechanical tests which are covered by ASTM Standard Test Methods, the high rate fracture toughness of material from each "plane" was measured. The test methodology is derived from the procedures for static rate testing (using a multiple specimen approach) and meets all the qualification requirements except that the loading rate allowed by the ASTM Standard Test Method is exceeded (the time to reach 40% of the maximum load must be in the range of 0.1 to 10 min to meet E 813-87 [4]; the time to 40% of the peak load in the high rate tests was less than 0.5 msec). The precision control required to perform high loading rate elastic-plastic testing is provided by special fixturing which limits both the displacement and maximum load during each individual test. A complete description of the test technique is reported elsewhere [5,6]. The measured values for the high rate fracture toughness are reported in Table I. The loading rate applied during the high rate fracture toughness tests surpassed that measured during the actual drop test (the time to peak load in the laboratory tests was ~0.75 msec, while the time to peak load during the actual drop test was ~1.4 msec). Fracture toughness measurements were conducted at -20°F. For this material (as well as many other ferritic alloys) the fracture toughness decreases with increasing loading rate and decreasing temperature. The laboratory testing conditions, with respect to temperature and loading rate, were thus conservative (i.e. lower in temperature and higher in loading rate) compared to the conditions experienced by the cask during the drop test. The size of the laboratory specimens were not conservative compared to the dimensions of the cask and it is possible that the increased dimensional constraint present in the vicinity of the flaw in the cask can cause the fracture toughness to be lowered. The sequence of additional drop tests that are planned for the MOSAIK KfK will determine if there is an effect of size on the fracture toughness.

The microstructure of the bottom coring does not precisely match the microstructure of small (1 inch) corings taken from the sidewalls. The manufacturing methods used to cast and subsequently cool the MOSAIK KfK caused this difference. It is important to note that the variation in the microstructure of the bottom coring exceeds that found in the sidewall material (due to the specific casting procedure). The total sidewall microstructural variation is limited to that found in Planes 1 through 3 in the bottom coring. The mechanical properties (strength, ductility, and fracture toughness) of the sidewall (which control the structural response for the side-drop orientation) has thus been estimated from the properties of Planes 1 through 3. These

\* Although not reported on here, Charpy impact tests were conducted as a function of temperature, and the elastic constants were determined from ultrasonic velocity measurements at room temperature. A complete description of all of the mechanical testing can be found in an earlier report(5).

## Mosaik Drop Test Program

### Flaw Characteristics

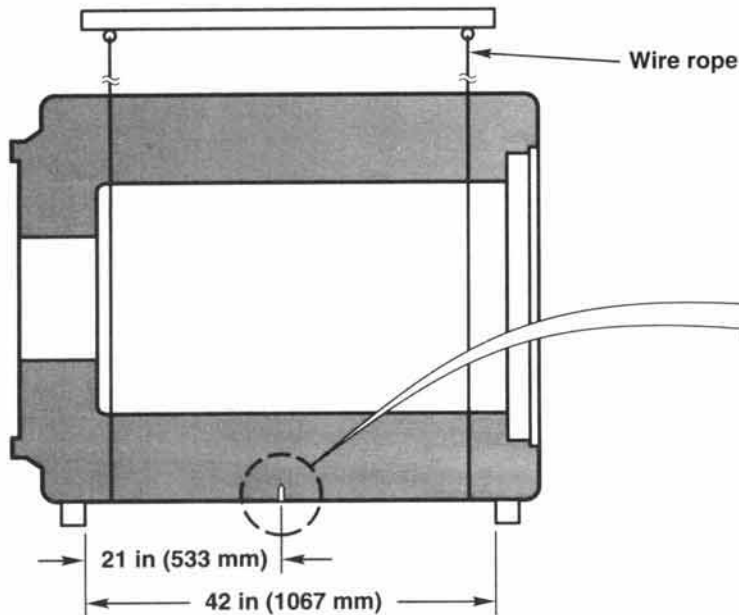


Fig. 1a. Schematic of Mosaik KfK Cask.

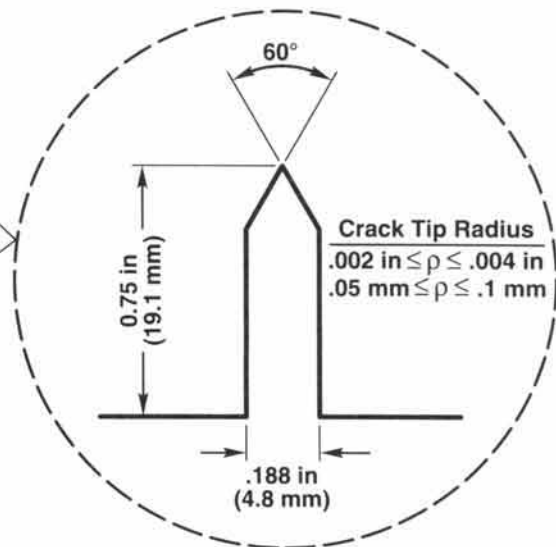


Fig. 1b. Schematic of flaw.

mechanical properties were used in the structural analysis to predict the behavior of the MOSAIK KfK during the 30 ft drop test. Once the full series of drop tests on this cask has been completed, mechanical test specimens as a function of location will be machined from sidewall material, and these specimens will be tested to quantify how well the sidewall properties were estimated from the bottom coring measurements.

### STRESS ANALYSIS

While the closure end of the cask differs from the opposite end, the cask ends are similar enough that the plane of the flaw can be considered a plane of symmetry. A second plane of symmetry was taken along the longitudinal axis of the crack through the center of the flaw. Thus, only one-fourth of the cask was included in the finite element model.

The flaw tip was modeled using standard 8-node hexahedral (brick) elements with one face collapsed to a line, which resulted in triangular prisms. All eight nodes of each flaw tip element were retained, with the two nodes on each end of the collapsed face starting at coincident locations. These initially coincident nodes were allowed to displace independently, resulting in a strain singularity at the flaw tip. Four elements were used around the 180° arc from

the flaw face to the plane of symmetry. This results in a fan-shaped mesh around the flaw.

A relatively fine mesh was employed in the region around the flaw. A transition to a much more coarse mesh away from the flaw was accomplished using *tied surfaces*. A *tied surface* maintains the relative locations of nodes from one surface to another. This technique permits rapid transitions in mesh refinement without allowing gaps, overlaps, or relative translation. The impact-enhancing rails were attached to the cask body using this technique.

The drop test was simulated by imposing a rigid surface at the bottom of the rails. The entire model (cask and rails) was given an initial velocity toward the rigid surface equivalent to that which would result from a thirty foot free fall. Thus the start of the analysis coincides with the initial impact of the cask onto the unyielding target. PRONTO3D [7] was used to perform the nonlinear transient dynamic analysis of this event.

### INSTRUMENTATION

The MOSAIC KfK was instrumented with accelerometers and strain gages to measure deceleration and surface strain. Endevco[8] model 7270A-6K and 7270A-20K accelerometers were mounted at various locations along and around the interior cavity of the test unit. The cask was also

TABLE I

A Summary of the Compositional/Microstructural Values and the Mechanical Properties Measured (at -30°C) for the Bottom Coring from the MOSAIK KfK Cask

| Sample Location | Graphite Vol. Fract. (%) | Pearlite Vol. Fract. (%) | Nodule Count (#/in <sup>2</sup> ) | Nodule Spacing (in)   | Nodule Type               | Ferrite Grain Size (in) | C (wt.%) | Si (wt.%) | Ni (wt.%) | S (wt.%) |
|-----------------|--------------------------|--------------------------|-----------------------------------|-----------------------|---------------------------|-------------------------|----------|-----------|-----------|----------|
| Plane 1         | 10.5                     | 0                        | 7.94x10 <sup>4</sup>              | 1.77x10 <sup>-3</sup> | 100% type I               | 1.18x10 <sup>-3</sup>   | 3.56     | 1.72      | 0.06      | 0.006    |
| Plane 2         | 13.8                     | 0                        | 7.87x10 <sup>4</sup>              | 1.77x10 <sup>-3</sup> | 100% type I               | 1.14x10 <sup>-3</sup>   |          |           |           |          |
| Plane 3         | 10.8                     | 3                        | 4.77x10 <sup>4</sup>              | 2.28x10 <sup>-3</sup> | 100% type I               | 1.14x10 <sup>-3</sup>   | 3.39     | 1.74      | 0.06      | 0.005    |
| Plane 4         | 18.4                     | 3                        | 2.65x10 <sup>4</sup>              | 3.11x10 <sup>-3</sup> | 90% type I<br>10% type II | 1.34x10 <sup>-3</sup>   |          |           |           |          |
| Plane 5         | 18.0                     | 5                        | 3.10x10 <sup>4</sup>              | 2.87x10 <sup>-3</sup> | 75% type I<br>25% type II | 1.46x10 <sup>-3</sup>   | 3.32     | 1.70      | 0.06      | 0.005    |

| Sample Location | Tensile Data                     |                      |                         |                  |                       | Static Fracture Tough.  |   | High Rate Frac. Tough.  |   |
|-----------------|----------------------------------|----------------------|-------------------------|------------------|-----------------------|-------------------------|---|-------------------------|---|
|                 | Strain Rate (sec <sup>-1</sup> ) | Yield Strength (ksi) | Ultimate Strength (ksi) | Total Elong. (%) | Reduction in Area (%) | J <sub>0</sub> (in-psi) | K <sub>J</sub> (ksi-in <sup>1/2</sup> ) | J <sub>0</sub> (in-psi) | K <sub>J</sub> (ksi-in <sup>1/2</sup> ) |
| Plane 1         | 10 <sup>-3</sup>                 | 34.5                 | 54.9                    | 26.9             | 22.6                  | 309                     | 86.6                                    | 188                     | 67.6                                    |
|                 | 10 <sup>0</sup>                  | 44.1                 | 59.6                    | 25.6             | 19.4                  |                         |   |                         |   |
| Plane 2         | 10 <sup>-3</sup>                 | 35.2                 | 55.4                    | 25.0             | 21.9                  | 310                     | 86.8                                    | 187                     | 67.5                                    |
|                 | 10 <sup>0</sup>                  | 43.6                 | 60.0                    | 18.3             | 20.8                  |                         |   |                         |   |
| Plane 3         | 10 <sup>-3</sup>                 | 36.1                 | 53.9                    | 21.0             | 17.0                  | 312                     | 86.6                                    | 197                     | 68.8                                    |
|                 | 10 <sup>0</sup>                  | 43.0                 | 56.2                    | 16.2             | 15.4                  |                         |   |                         |   |
| Plane 4         | 10 <sup>-3</sup>                 | 36.1                 | 53.5                    | 14.3             | 14.3                  | 319                     | 87.1                                    | 105                     | 49.9                                    |
|                 | 10 <sup>0</sup>                  | 42.5                 | 56.6                    | 13.5             | 10.5                  |                         |   |                         |   |
| Plane 5         | 10 <sup>-3</sup>                 | 36.3                 | 54.7                    | 15.7             | 15.0                  | 336                     | 89.2                                    | 110                     | 51.0                                    |
|                 | 10 <sup>0</sup>                  | 44.8                 | 60.0                    | 21.4             | 15.0                  |                         |   |                         |   |

instrumented with seventeen biaxial CEA06-25OUT-350 strain gages from Measurement Groups[9]. The complete instrumentation package was designed to capture the entire cask response, to provide appropriate measurement redundancy for data verification and to benchmark the stress analysis.

## RESULTS

The acceleration and strain gage data were acquired using the Mobile Instrumentation Data Acquisition System (MIDAS)[10]. The system includes all equipment necessary to acquire and process impact and thermal data. The accelerometer and strain gage data were recorded digitally at a rate of 500,000 samples per second. The data were transferred to the systems digital computer for data analysis. The presentation of the data focuses on the initial impact of the cask. The peak accelerations, filtered at 500HZ, are shown in Fig. 2. The maximum measured accelerations occurred at the ends of the cask due to the increased stiffness (relative to the middle of the cask) in this area. The measured acceleration in the vicinity of the flaw was 510 gs. Using the accelerometer data, the measured time to peak load ranges from 2.9 to 4.1 msec, depending on location of the accelerometer on the cask.

The peak strains from selected strain gages are shown in Fig. 2. The peak axial outside surface strains ranged from

700 to 1400 microstrain. The peak hoop strains on the cask outer surface ranged from 440 to 1400 microstrain. Using the strain gage data, the measured time to peak values is approximately 2.6 msec. All the strain gage measurements remained elastic, regardless of location on the cask. A small amount of permanent deformation occurred at the interface of the steel rails with the cask.

The finite element analysis showed that the behavior of the cask was nominally elastic during the drop test, with a small region of localized plasticity at the steel rails. Perhaps the best measure of the nominal cask behavior are the strains at gage locations S11 and S13. Strain gages S11 and S13 are located symmetrically on either side of the notch, and are close enough to the notch to capture the nominal stress field, while being sufficiently far away to avoid the local perturbations associated with the notch. The measured strain - time history is compared to the computed values at these locations in Fig. 4. The magnitudes of the peak strains are comparable, but the measured time to peak strain is longer than the computed time. This difference has not yet been reconciled, but it could be due to the slight secondary impact ("slapdown") experienced by the cask (i.e., one end made contact with the target ~0.1 milliseconds before the other end).

The J-integral was calculated along the notch front using the computed stresses and displacements from the



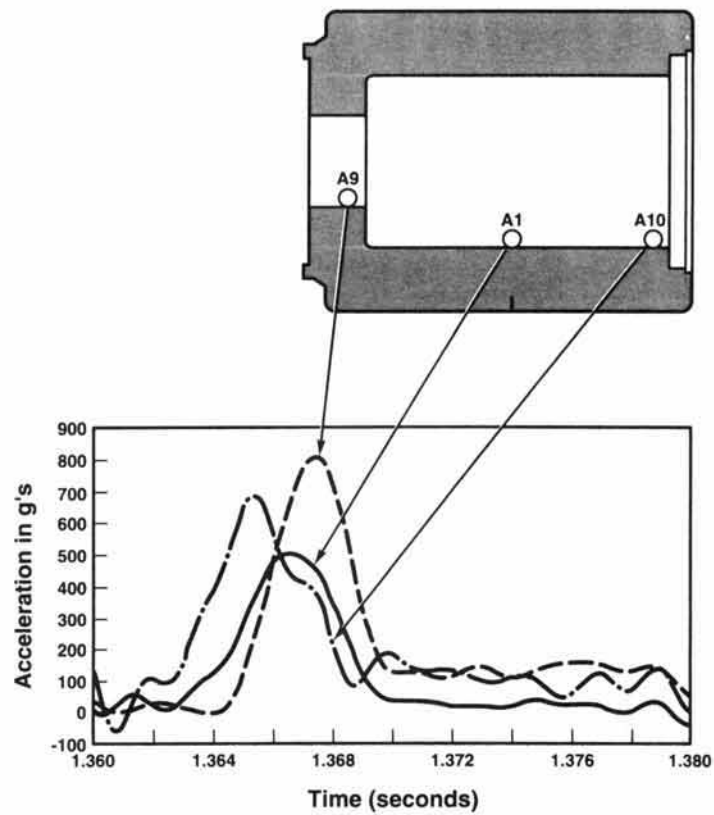


Fig. 2. Peak accelerations for selected accelerometers.

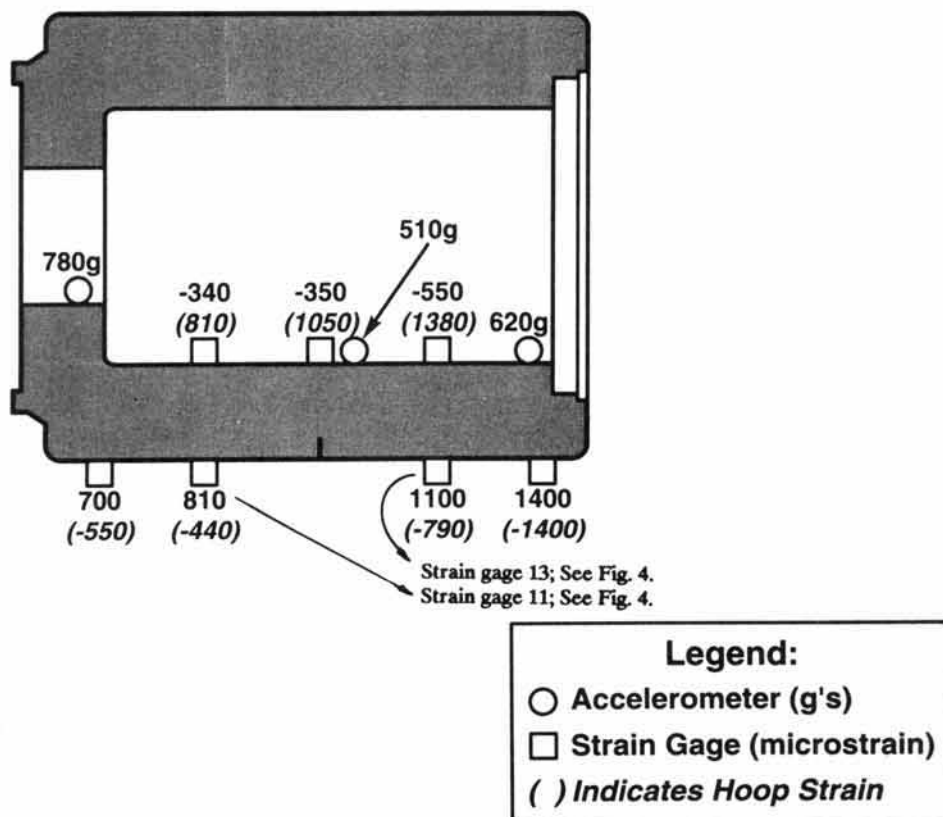


Fig. 3. Selected instrumentation and peak values.

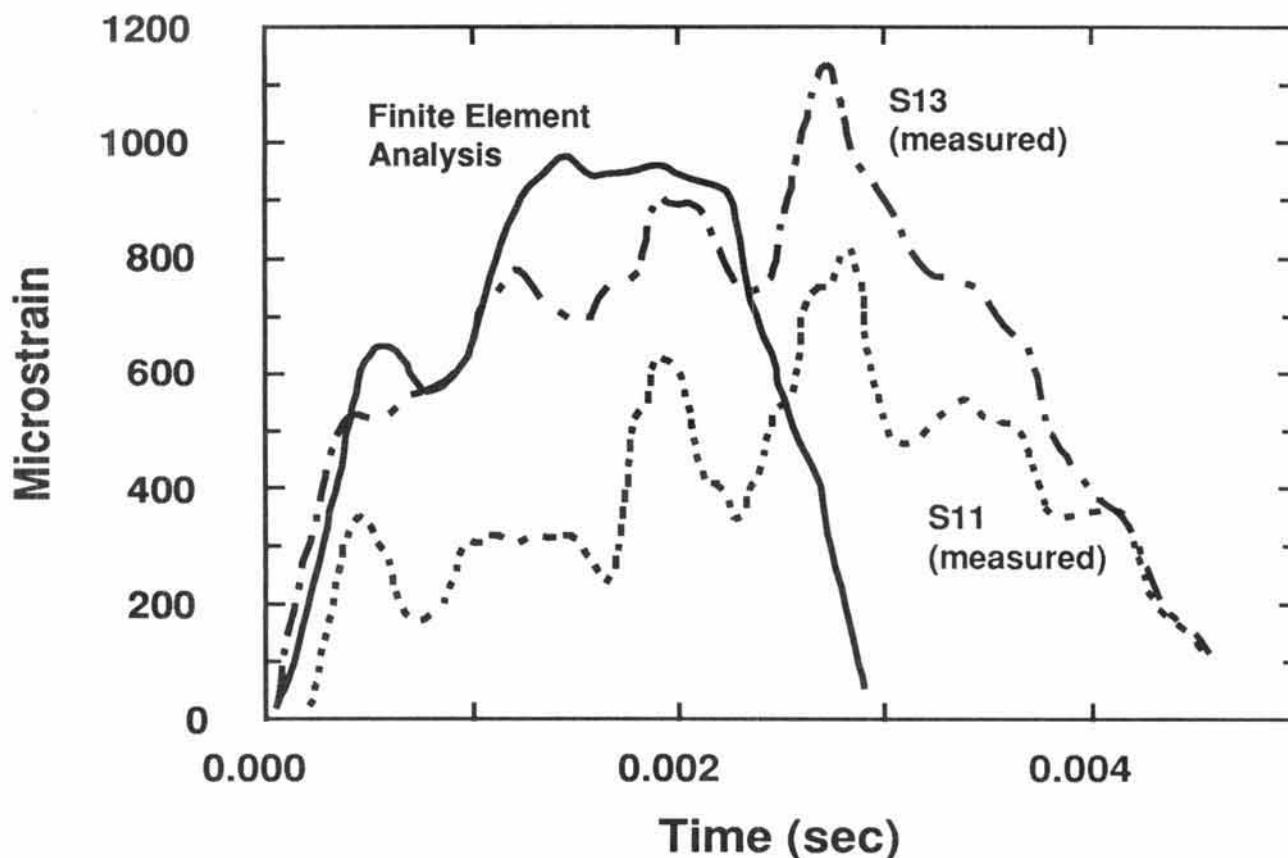


Fig. 4. Comparison between calculated (finite element analysis) and measured strains.

finite element analysis. As expected, the J-integral took its highest value at the deepest point of the notch. The stress intensity factor, estimated from this J value was  $46 \text{ ksi-in}^{1/2}$ ; similar to the  $42 \text{ ksi-in}^{1/2}$  calculated using linear elastic fracture mechanics (as described earlier) with a nominal stress of 26 ksi. Table II summarizes the comparison between measured data and calculated values.

The tip of the flaw was scanned with an optical probe to determine whether a crack had initiated. In addition, the ends of the machined flaw that intersected the surface were examined for evidence of crack extension. No evidence of crack extension was noted. This verifies that the applied stress intensity,  $K_I$ , was less than the fracture toughness,  $K_{Ic}$ , of the cask material.

### CONCLUSIONS

This drop test provides a practical demonstration of how the fracture mechanics design approach can be applied to nuclear material transport casks. As a result, this test program verifies the methodology by which materials other than austenitic stainless steels can be properly evaluated for use as a containment boundary in transport casks.

For the conditions of this drop test, no crack initiation was predicted and the test results verified that this was in fact the case. Additional tests are planned to force crack

initiation in order to quantify the margin of safety and to verify the laboratory measurements of fracture toughness.

An important part of the fracture mechanics approach is the calculation of stresses in the cask body. The difference between calculated and measured strains was shown to be approximately 10%. The variation in correlation was most probably due to the effects of the asymmetrical impact of the ends of the cask. The drop test demonstrates that the finite element analysis adequately estimated stresses, given the experimental accuracy of materials testing, control of the drop test, and data acquisition during the drop event.

Although the margin of safety could not be quantified from this first test, the lack of any crack initiation resulting from the drop test provides a measure of confidence that the LEFM design methodology is appropriate for this application. The subsequent drop tests are designed to quantify the margin of safety. All the drop tests in this program will exceed the test requirements specified in 10CFR 71 by providing a significant flaw in the cask body and by enhancing the effect of the impact through the use of the steel rails. The severe impact conditions (relative to 10CFR71) provide an additional degree of conservatism since the regulatory drop test conditions do not induce a sufficient level of stress nor the proper stress gradient (i.e. through wall tensile stress) to drive a crack through the wall.

## REFERENCES

1. "ASTM A 874--89: Specification for Ferritic Ductile Cast Iron Castings Suitable for Low Temperature Service," *1990 Annual Book of ASTM Standards, Section 1, Ferrous Castings, Ferroalloys; Ship Building, 1.02*, American Society for Testing and Materials, Philadelphia, 1990, pp. 493-495.
2. *Code of Federal Regulations, Title 10, Part 71*, "Packaging for Transportation of Radioactive Material, August 1983.
3. "ASTM E 23-88: Standard Test Methods for Notched Bar Impact Testing of Metallic Materials," *1989 Annual Book of ASTM Standards, Section 3, Metals Test Methods and Analytical Procedures, 3.01*, American Society for Testing and Materials, Philadelphia, 1989, pp. 198-213.
4. "ASTM E 813-87: Standard Test Method for  $J_{IC}$ , A Measure of Fracture Toughness," *1989 Annual Book of ASTM Standards, Section 3, Metals Test Methods and Analytical Procedures, 3.01*, American Society for Testing and Materials, Philadelphia, 1989, pp. 698-712.
5. R. SALZBRENNER and T. B. CRENSHAW, "Mechanical Property Mapping of the Ductile Cast Iron MOSAIK KfK Cask," *SANDIA REPORT SAND90-0776 • UC-512*, Sandia National Laboratories, Albuquerque, NM, Aug. 1990.
6. R. SALZBRENNER and T. B. CRENSHAW, "Multiple Specimen J Integral Testing at Intermediate Rates," *Experimental Mechanics*, Sept. 1990, p 217.
7. L. M. TAYLOR and D. P. FLANIGAN, "PRONTO 3D A Three Dimensional Transient Solid State Dynamics Program," *SANDIA REPORT SAND87-1912*, Sandia National Laboratories, Albuquerque, New Mexico, March 1989.
8. ENDEVCO, 30700 Rancho Viejo Road, San Juan Capistrano, CA, 92675.
9. Measurements Group Inc. MICRO-Measurements Division, Raleigh, North Carolina.
10. W. L. UNCAPHER, et. al., "The Development of the Mobile Instrumentation Data Acquisition System, for Use in Cask Testing," *Proceedings of the Ninth International Symposium on Packaging and Transportation of Radioactive Material: PATRAM 89*, Washington, D.C.